

Article

Numerical Simulation of the Heat Transfer Inside a Shell and Tube Heat Exchanger Considering Different Variations in the Geometric Parameters of the Design

José Estupiñán-Campos ¹, William Quitiaquez ^{1,2,*} , César Nieto-Londoño ³  and Patricio Quitiaquez ^{2,4}

¹ Department of Mechanical Engineering, Universidad Politécnica Salesiana, Quito EC170525, Ecuador; jestupinanc@est.ups.edu.ec

² Productivity and Industrial Simulation Research Group (GIIPSI), Department of Master's Degree in Production and Industrial Operations Engineering, Universidad Politécnica Salesiana, Quito EC170525, Ecuador; rquitiaquez@ups.edu.ec

³ Escuela de Ingenierías, Universidad Pontificia Bolivariana, Medellín CO050031, Colombia; cesar.nieto@upb.edu.co

⁴ Department of Mechatronics Engineering, Universidad Politécnica Salesiana, Quito EC170525, Ecuador

* Correspondence: wquitiaquez@ups.edu.ec

Abstract: The present study aims to analyze the heat transfer variations in different models of shell and tube heat exchangers considering geometric variations in the baffle angles and in the tube's profiles. Each baffle configuration and geometric variation in the profiles were tested under different mass flow rates (0.25, 0.5, 0.75, and 1 kg·s⁻¹) in the shell to study the heat transfer improvement. The models were simulated using a CFD simulation software ANSYS Fluent including an experimental geometry which was used to validate the simulation process. The experiment results are in good agreement with the CFD results. The analysis of the results shows that an angle of 60° in the baffles generated the highest heat flow (more than 40 kW) with an inclination to the cold flow inlet and a mixed distribution considering a mass flow rate of 1 kg·s⁻¹ in the shell. In addition, the horizontal elliptic profile achieved a heat flow higher than 29 kW with a mass flow rate of 0.5 kg·s⁻¹ in the shell.

Keywords: shell and tube heat exchangers; heat transfer; baffle; profiles; CFD



Citation: Estupiñán-Campos, J.; Quitiaquez, W.; Nieto-Londoño, C.; Quitiaquez, P. Numerical Simulation of the Heat Transfer Inside a Shell and Tube Heat Exchanger Considering Different Variations in the Geometric Parameters of the Design. *Energies* **2024**, *17*, 691. <https://doi.org/10.3390/en17030691>

Academic Editor: Artur Bartosik

Received: 31 December 2023

Revised: 18 January 2024

Accepted: 24 January 2024

Published: 31 January 2024



Copyright: © 2024 by the authors. Licensee MDPI, Basel, Switzerland. This article is an open access article distributed under the terms and conditions of the Creative Commons Attribution (CC BY) license (<https://creativecommons.org/licenses/by/4.0/>).

1. Introduction

Currently, heat exchange processes between fluids have gained great notoriety in industries such as electronics, aerospace, chemical, refrigeration, and in various modern engineering applications due to the high energy consumption they can generate. For this reason, the efficient use of energy is an alternative to reduce the scarcity of this resource worldwide, and it can be achieved using any type of energy-saving technique [1]. These techniques can involve algorithms to perform the calculation, and the comparison of thermal machine parameters, as presented by Mediaceja et al. [2].

In the case of shell and tube heat exchangers, efficient energy management can be carried out by considering more appropriate values for various design parameters, satisfying the energy needs and producing the best thermo-hydraulic behavior according to the objective function [3,4].

As a result of the numerical analysis, it is possible to obtain a large number of variables of interest to relate the behavior of the working fluids and thermal energy transfer. In this line of research, Ravikumar and Raj [5] present the effects of parameters such as temperature variation and pressure drop to establish a relationship with the heat flow and efficiency generated by changes in a shell and tube heat exchanger.

Due to the importance that the optimization of heat exchangers represents in this field, authors such as Pereira et al. [6] and Yang et al. [7] continue with the trend to redesign these systems with programming aimed at guiding, with certain guidelines, the development of

models with greater efficiency and an adequate verification process. In this context, the work of Li et al. [8] stands out, where a change in the traditional design of the tube with circular profile for a tube with a twisted section was proposed, increasing the performance of the heat flow between 24 and 39%.

In this field, numerical analysis is used to determine the transport of thermal energy in a shell and tube heat exchanger (TC exchanger). Using this method, it is possible to establish the influence of the thermodynamic properties of various working fluids, as presented by Bahiraei et al. [9], where a three-dimensional model of the exchanger was generated and the passage of nanofluids was simulated to determine the temperature variation, generating a maximum increase of 13 °C when considering nanoparticles with different geometric shapes.

In this context, the study of improvements in the efficiency of heat exchange devices has been presented in research works such as the one developed by Abbasian and Uosofvand [10]. This work studies the variation in heat transfer between fluids by incorporating geometric modifications in the profile of the tube and baffle, using computational fluid dynamics (CFD) analysis, with an increase of 20.9% using an optimized tube with an elliptical angled arrangement.

Ren et al. [11] performed a numerical and experimental analysis of a thermal energy storage device using a shell and tube heat exchanger system, implementing changes in the tube layout to determine the variation in heat exchanger efficiency due to the influence of parameters such as tube diameter, tube length, flow rate, and tube layout, among others. In this way, they generated a sensitivity index of 0, 0.215, 0.2, and 0.35, respectively, quantifying the effects of the input variables (geometric changes) on the response (heat transfer) of the interaction of their effects.

CFD analysis as a method to study the transport of thermal energy in the working fluids in CT heat exchangers is widely used to determine pressure drops, changes in the heat transfer coefficient, and Nusselt and Reynolds numbers, as shown in the study by Quitiaquez et al. [12] and in the research developed by Li et al. [13]. In the latter, a numerical analysis was performed together with an experimental study varying the baffles of the device, to generate a maximum pressure drop inside the shell between 700 and 6500 Pa approximately, with a verification process showing a variation of 9.10 and 5.32%.

In this field of study, it is possible to relate the increase in heat flux to the improvement in heat transfer coefficient, device effectiveness, and the number of units transferred (NTU). In the study by Said et al. [14], the authors elaborated a numerical analysis of a TC exchanger with three geometric changes in the baffles, obtaining as maximum values and effectiveness of 0.37, an NTU of 0.625, and a maximum global heat transfer coefficient of $315 \text{ W}\cdot\text{m}^{-2}\cdot\text{K}^{-1}$, among others. The results showed an average variation between the global heat transfer coefficient and pressure drop of 8.44 and 8.77%, respectively, when comparing the experimental values with those obtained in the numerical analysis.

In order to improve the thermal effectiveness of the energy transfer devices, Biçer et al. [15] proposed a change in the design of the baffles to reduce the pressure drop on the shell walls while maintaining the thermal effectiveness of the heat exchanger. The generated model caused a pressure drop of less than 49%, with an increase in the tube surface temperature of 7%, using computational fluid dynamics analysis, compared with experimental results which showed a variation of 7.3%.

Nagib et al. [16] employed CFD simulations to evaluate a cross-flow heat exchanger incorporating partition plates to reduce the pressure drop by 20% and increase the Nusselt number, leading to an increase in the heat transfer coefficient of 7% considering flow regimes of 5500 and 14,500. To validate the outlet temperature of heat exchangers with various mass flow rates, Vivekanandan et al. [17] performed a CFD analysis, with experimental results showing a similar trend to those obtained in the numerical analysis, with an error of 15% and an overall heat transfer coefficient of $449.2 \text{ W}\cdot\text{m}^{-2}\cdot\text{K}^{-1}$. A similar development can be seen in works such as the one developed by Krishna et al. [18], when comparing the results obtained by numerical analysis with experimental results, with a variation of 5.32%,

studying the temperature difference along the heat exchanger device with a mass flow rate between 0.05 and 0.25 kg·s⁻¹.

A similar validation was developed in the research of Aliaga et al. [19], showing a difference of less than 6.2% between the experimental results and those obtained by CFD in an optimized heat exchanger prototype to achieve an efficiency of 95%. A study developed on changes in geometrical design parameters in shell and tube heat exchangers with baffle plates connected to a central tube, showed results with a variation of 15% between the experimental model and the numerically analyzed one, with a maximum efficiency of 0.775 with flow rates between 2 and 6 lpm in the tube, together with values between 2 and 8 lpm in the shell of the device [20].

The present research work aims to perform a CFD analysis in ANSYS 2023 R1 of the behavior of the fluids in a heat exchanger that presents geometric design variations to determine the arrangement that generates a greater temperature variation between the inlet and outlet of the working fluids in the device, resulting in an increase in the heat flow. In the introduction, a review of the research that has been carried out in this field is presented, and the CFD analysis process is subsequently addressed in the materials and methods section. Finally, the results obtained for each model analyzed are shown together with the most relevant conclusions that they generated.

2. Materials and Methods

In the present study, a comparative analysis was performed with the temperature variation in the working fluids at the ends of the shell and tube heat exchanger. This study considered a base case in which geometrical changes in the ducts and baffles were incorporated. The temperature variations were determined by means of a CFD analysis process that started by creating the designs within a modeling software, then the meshing was generated, which in turn involved a mesh independence analysis and quality verification. Subsequently, the simulation parameters were entered, the mathematical calculation models were selected, and the results were obtained and compared with the proposed base case, as shown in Figure 1.

2.1. Parameters for Analysis

In order to develop the analysis of the thermal energy transfer between the working fluids in the various models of the proposed heat exchanger, several operability factors were considered, as presented in Table 1, to establish values for comparison with a base case.

Table 1. Exchanger operating conditions.

	Input Parameters Mass Flow Rate [kg·s ⁻¹]	Temperature Inlet [°C]
Cold fluid	0.25, 0.5, 0.75, 1	20
Hot fluid	0.3	70

Similarly, to perform the CFD analysis, the thermodynamic properties of the working fluid (water) and the material of the heat exchange devices were considered, as shown in Table 2.

Table 2. Exchanger operating conditions 2.

Water				
Temperature [°C]	Density [kg·m ⁻³]	Thermal Conductivity [W·m ⁻¹ ·K ⁻¹]	Specific Heat Capacity [J·kg ⁻¹ ·K ⁻¹]	Dynamic Viscosity [kg·m ⁻¹ ·s ⁻¹]
20	998.2	0.5861	4183	0.001002
30	995.7	0.603	4183	0.0007977
40	992.2	0.6178	4182	0.0006533

Table 2. Cont.

Water				
Temperature [°C]	Density [kg·m ⁻³]	Thermal Conductivity [W·m ⁻¹ ·K ⁻¹]	Specific Heat Capacity [J·kg ⁻¹ ·K ⁻¹]	Dynamic Viscosity [kg·m ⁻¹ ·s ⁻¹]
50	988	0.6305	4181	0.0005471
60	983.2	0.641	4183	0.0004666
70	977.8	0.6495	4187	0.0004041
Copper				
Density [kg·m ⁻³]	Thermal Conductivity [W·m ⁻¹ ·K ⁻¹]	Specific Heat Capacity [J·kg ⁻¹ ·K ⁻¹]		
8978	387.6	381		

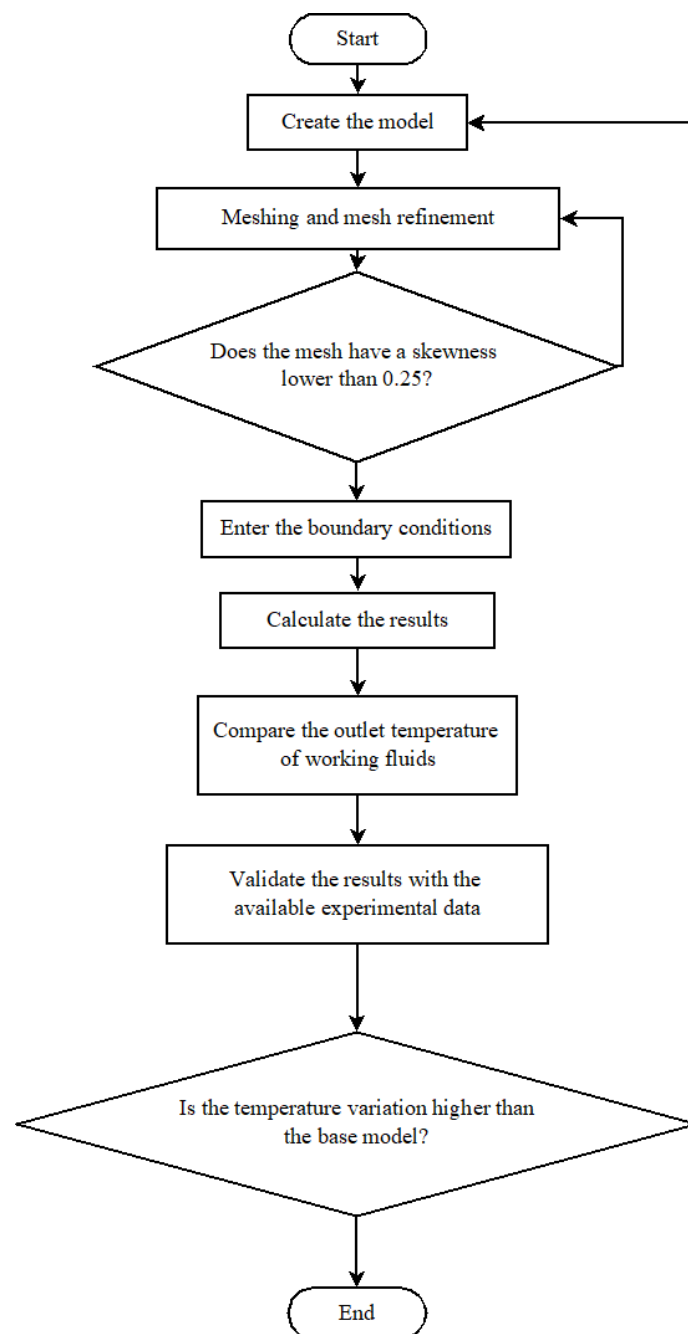


Figure 1. Flow chart of the simulation process.

2.2. CFD Analysis

Computational fluid dynamics analysis was used to determine the heat transfer in the various models of shell and tube heat exchangers proposed, which presented results such as the temperature at the outlets of the device and the surface temperature in the ducts.

2.3. Meshing

This research performed a numerical analysis of several models of shell and tube heat exchangers, starting from a base model that was selected through a comparative study with initial models that presented baffle walls with different heights. The mesh quality in each model was measured by skewness and is presented in Table 3.

Table 3. Exchanger operating conditions 3.

Model	Number of Elements Average	Skewness Average
Exchanger for validation	3,509,554	0.2899
Initial model 1 (baffles with 25% of the height)	467,003	0.238
Initial model 2 (baffles with 50% of the height)	471,875	0.2405
Starting model 3 (baffles with 75% of the height)	448,733	0.2417
Models with inclined baffle (30°)	471,552	0.2404
Models with inclined baffle (45°)	479,986	0.2406
Models with inclined baffle (60°)	500,137	0.2422
Inner tube models with arches and inclined baffles (60°)	483,386	0.2413
Elliptical (vertical) inner tube models with inclined baffles (60°)	497,216	0.2735
Elliptical (horizontal) inner tube models with inclined baffles (60°)	492,203	0.2767
Octagonal inner tube models with inclined baffles (60°)	495,627	0.253

In order to determine the convergence (average output temperature), the analysis of the base model was performed with different meshes that increased the number of elements, varying the mesh quality. Thus, it was shown that when exceeding 350,000 elements, the output temperature converges to 31.9 °C (Figure 2), validating the mesh quality used.

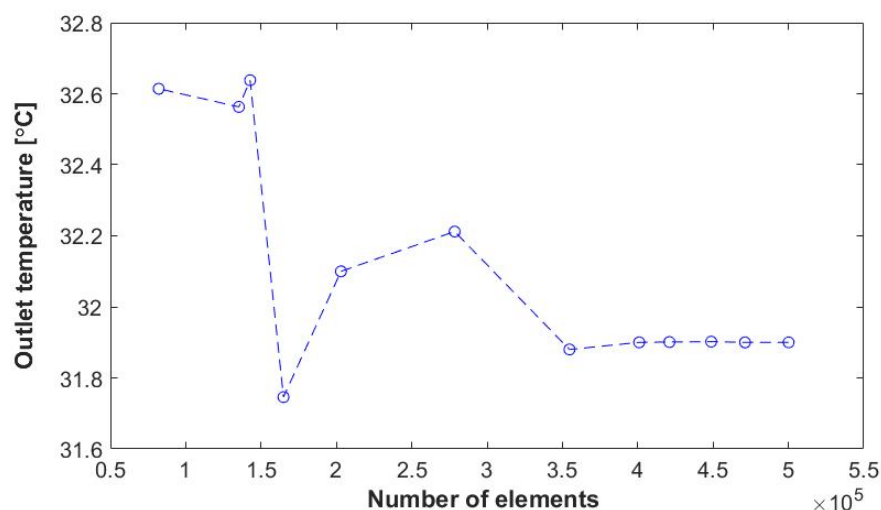


Figure 2. Convergence of the mesh in the exchanger (initial model 3).

The meshing of the analyzed models presented tetrahedral elements that adapted to the curvatures of the ducts, as in the case of the initial model 3 shown in Figure 3.

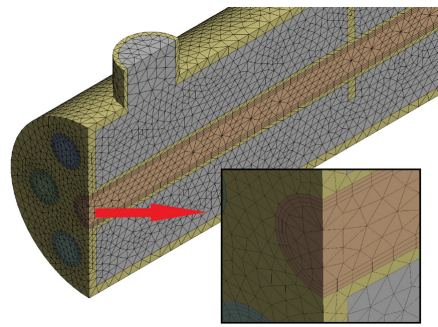


Figure 3. Initial model 3 meshing.

2.4. Governing Equations

Navier–Stokes equations, which involve the conservation of continuity (mass), the quantity of motion, and energy, as seen in Equations (1), (2), and (3), respectively, were used to determine the behavior of the working fluids during the heat exchange [21,22]. Mathematical models can be selected according to the characteristics of the study to calculate the influence of the conditions in the heat transfer process through walls, as it was presented in the work of Chihab et al. [23].

$$\frac{\partial \rho}{\partial t} + \nabla \cdot (\rho \vec{V}) = S_m \tag{1}$$

$$\frac{\partial}{\partial t} (\rho \vec{V}) + \nabla \cdot (\rho \vec{V} \vec{V}) = -\nabla P + \nabla \cdot (\bar{\tau}) + \rho \vec{g} + \vec{F} \tag{2}$$

$$\frac{\partial}{\partial t} (\rho E) + \nabla \cdot [\vec{V} \cdot (\rho E + P)] = -\nabla \cdot \left(\sum_j h_j J_j \right) + S_h \tag{3}$$

In order to study the behavior of the fluids in a turbulent state inside curved ducts, studies like the investigation of Wang and Suen [24] refer to turbulence models (the standard $k-\epsilon$ model, the RNG $k-\epsilon$ model with/without swirl option, and the standard $k-\omega$ model, among others) that produce an adequate similarity between simulated and experimental results. Considering the flow regime of the fluids in the present analysis, the turbulence model chosen was the standard $k-\epsilon$ turbulence model (Equations (4) and (5)), which allows us to obtain results with high accuracy according to the experimental data [25].

$$\frac{\partial}{\partial t} (\rho k) + \frac{\partial}{\partial x_i} (\rho k u_i) = \frac{\partial}{\partial x_j} \left[\left(\mu + \frac{\mu_t}{\sigma_k} \right) \frac{\partial k}{\partial x_j} \right] + G_k + G_b - \rho \epsilon - Y_M + S_k \tag{4}$$

$$\frac{\partial}{\partial t} (\rho \epsilon) + \frac{\partial}{\partial x_i} (\rho \epsilon u_i) = \frac{\partial}{\partial x_j} \left[\left(\mu + \frac{\mu_t}{\sigma_\epsilon} \right) \frac{\partial \epsilon}{\partial x_j} \right] + C_{1\epsilon} \frac{\epsilon}{k} (G_k + C_{3\epsilon} G_b) - C_{2\epsilon} \rho \frac{\epsilon^2}{k} + S_\epsilon \tag{5}$$

As part of the numerical analysis for the heat exchanger model, the pressure–velocity coupling scheme and the spatial discretization are presented in Table 4.

Table 4. Pressure–velocity coupling and spatial discretization.

Pressure–Velocity Coupling	
Schematic	Coupling
Spatial Discretization	
Pressure	Second order
Momentum	Second order
Energy	Second order
Kinetic energy turbulence	Second order
Turbulence dissipation rate	Second order

3. Results

The results obtained in the present study involve similar operating conditions in shell and tube heat exchanger devices that present geometrical variations from a base model to establish the changes in heat flow between the working fluids used.

3.1. Validation

To perform the validation of the computational fluid dynamics analysis in the heat exchange device, it is possible to compare the values of certain parameters as results obtained in the simulation with the experimental values in factors such as outlet temperature, effectiveness, or heat flow rate, with variations of the results between 5.32 and 15%, as presented in the research of Vivekanandan et al. [20] and Elgendy et al. [26], respectively.

For this reason, when comparing the experimental results obtained in the study of a shell and tube heat exchanger with different baffles developed by Biçer et al. [15] with a similar model simulated by the authors, it can be appreciated that an average error of 3.15% was obtained, as observed in the trend of Figure 4, validating the numerical analysis process used.

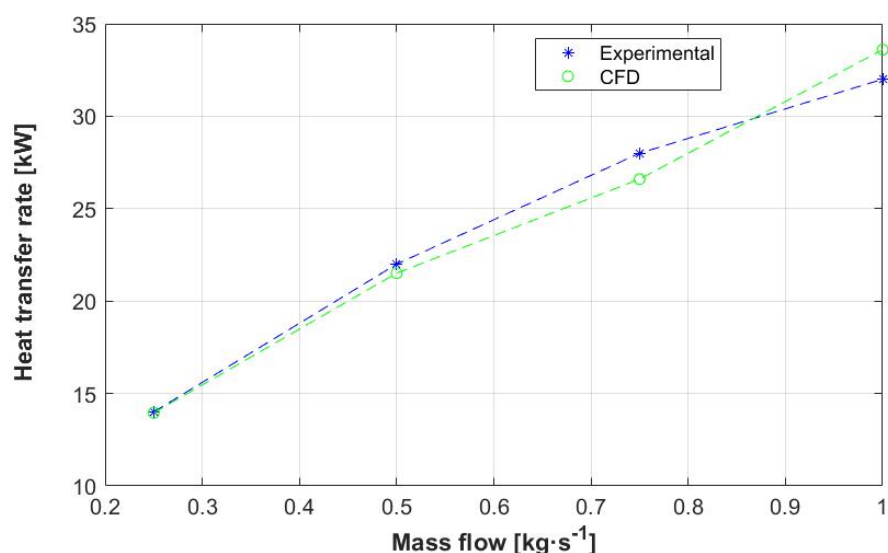


Figure 4. Heat transfer rates at different mass flow rates.

3.2. Base Model

A base model to establish an initial proposal was made for a shell and inner tubes, similar to the concept of the geometry used for the validation, as shown in the research work of Biçer et al. [15], with a reduced number of tubes and dimensions. The model's dimensions are presented in Table 5.

Table 5. Heat exchanger dimensions.

Length [m]	Internal Diameter of the Pipes [m]	External Diameter of the Pipes [m]	Internal Diameter of the Shell [m]	External Diameter of the Shell [m]	Distance between Tubes [m]	Internal Diameter of External Pipe [m]	Distance between Baffles [m]
0.35	0.008	0.010	0.038	0.042	0.012	0.012	0.07

In the proposed device, three initial models were considered where the baffle height was varied (25, 50, and 75%) concerning the inner diameter of the shell, in order to compare the variation in heat flux in each case in relation to the change in the average outlet temperature, as shown in Figure 5.

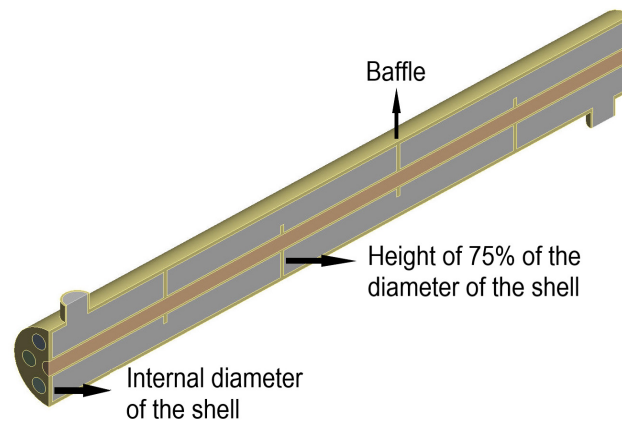


Figure 5. Initial model of the heat exchanger with 75% baffle height.

During the behavior analysis of the fluids in the initial models of the heat exchanger with baffles with 25% of the inner diameter of the shell (Model 1), 50% (Model 2), and 75% (Model 3), it was determined that the highest heat flow (related to the outlet temperature) occurred in Model 3, as can be appreciated in Figure 5 (part A), with a temperature change along the heat transfer device seen in Part B of Figure 6. For this reason, this model was selected as the base model.

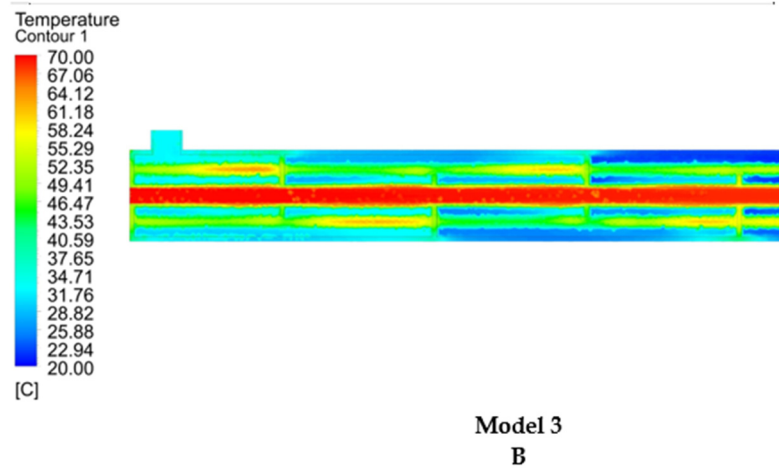
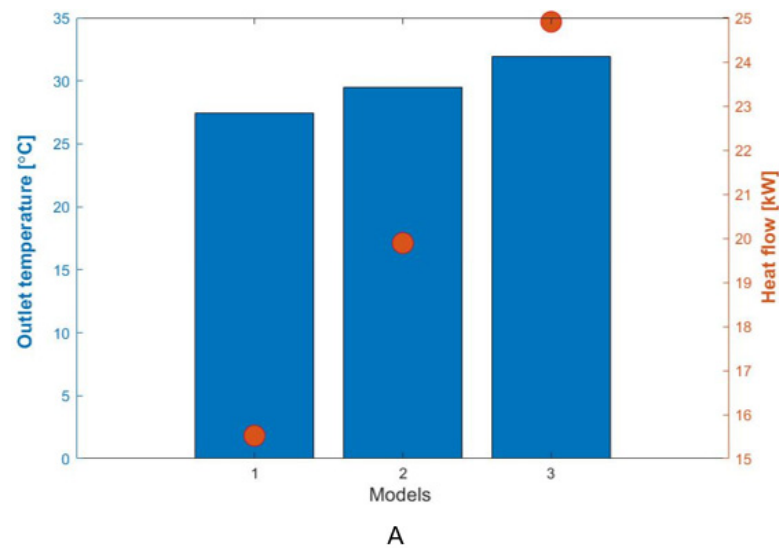


Figure 6. Change of temperature versus heat flow in the three models (A), and temperature contour in the heat exchanger section of Model 3 (B).

3.3. Changes in Inclination

From the base model, as a proposal to improve heat transfer, the considered geometries presented inclinations in the baffle walls varying their orientation for the inlet and outlet of the cold fluid, as was observed in several investigations [9,27].

3.3.1. Inclination of 30°

The behavior of the fluids in the heat exchanger was simulated by incorporating an inclination in the baffles of 30° concerning the vertical axis, where one end was directed toward the cold fluid outlet (A), the cold fluid inlet (B), and alternately (C), as shown in Figure 7.

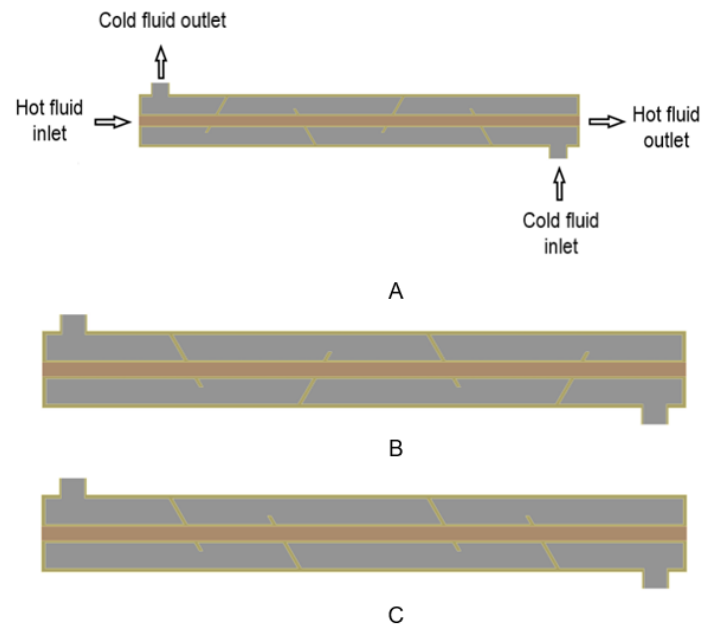


Figure 7. Heat exchangers with a 30° inclination in the baffles.

The 30° inclination of the baffle walls generated changes in the heat flux in the heat transfer device; when the results between the inclination cases considering different mass flow rates of the cold fluid were compared, it was determined that Case B results in a higher heat flux (39.3 kW) for a mass flow of 1 kg·s⁻¹, followed by the other cases and the base model, as shown in Figure 8. In addition, it can be seen that Case A generates the lowest heat flux, with a value of 15.44 kW for a mass flow of 0.25 kg·s⁻¹.

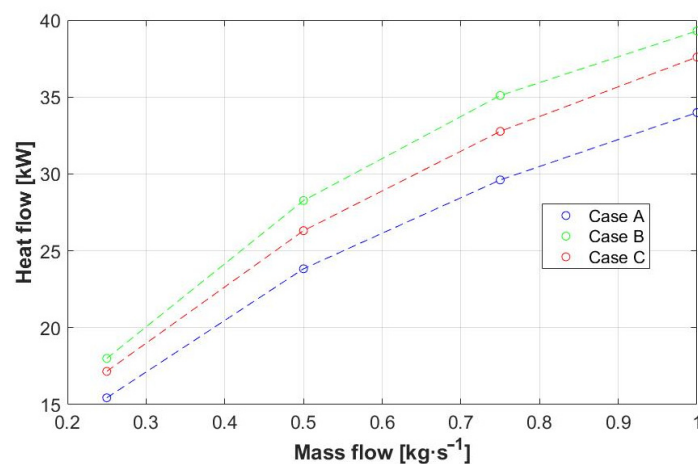


Figure 8. Heat flow for baffles with a 30° inclination in cases A, B, and C.

3.3.2. Inclination of 45°

Similarly, the behavior of the working fluid in the device was analyzed considering a 45° inclination of the baffles concerning the vertical axis, with one end oriented towards the cold fluid outlet (A), the cold fluid inlet (B), and alternately (C), as presented in Figure 9.

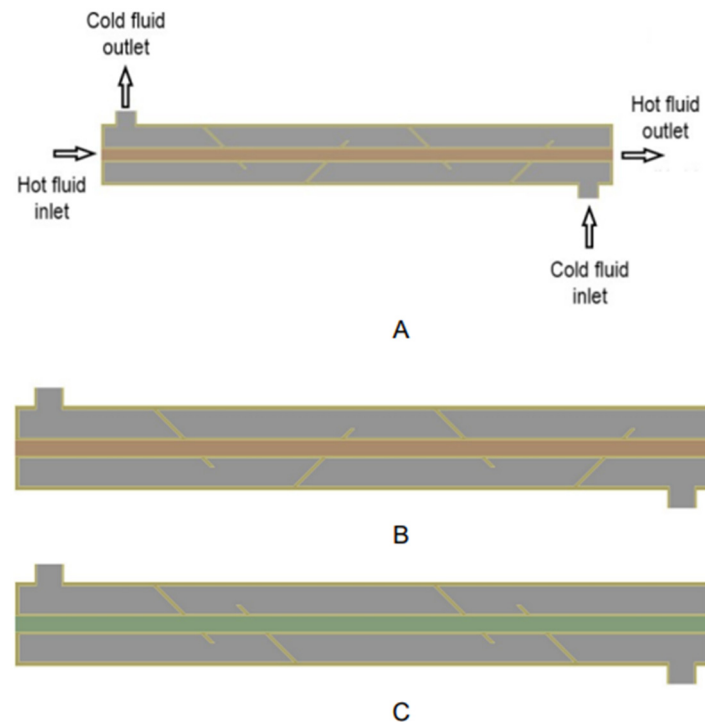


Figure 9. Heat exchangers with a 45° inclination in the baffles.

The study of the change in heat flow between the working fluids of the exchanger for an inclination of 45° for the different cases analyzed with various mass flows in the cold fluid, showed that Case B, when it was simulated with $1 \text{ kg}\cdot\text{s}^{-1}$, presented the highest heat transfer (40.03 kW) compared to the other cases and the base model, as shown in Figure 10. In this context, when a similar case was studied with the same mass flow, Case A generated the lowest heat flux (32.78 kW).

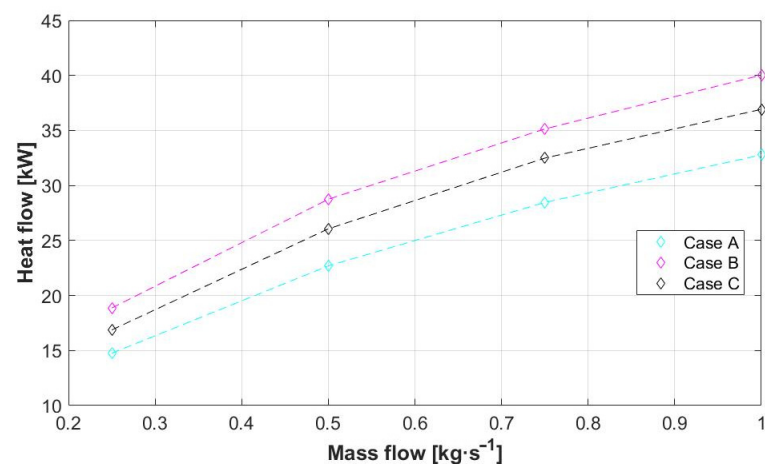


Figure 10. Heat flow for baffles with a 45° inclination in cases A, B, and C.

3.3.3. Inclination of 60°

Additionally, the analysis of the change in heat flow in the heat exchanger was performed by incorporating 60° inclinations in the baffles for the vertical axis along with end

orientations towards the cold fluid outlet (A), cold fluid inlet (B), and alternately (C), as shown in Figure 11.

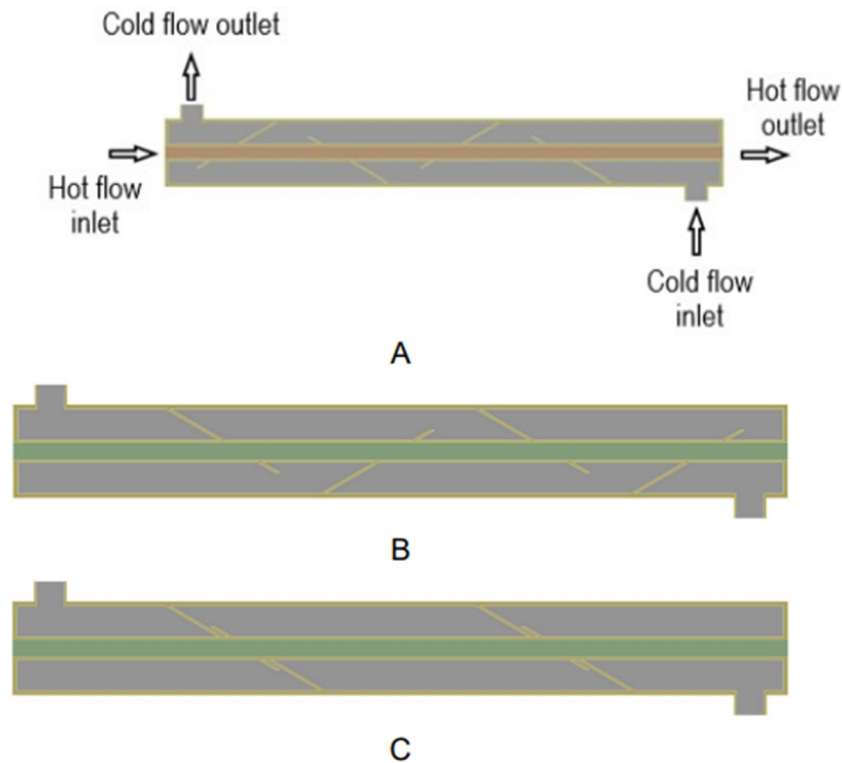


Figure 11. Heat exchangers with a 60° inclination in the baffles.

As a result of the simulation of the proposed cases, it was determined that both Cases B and C presented a notable increase in the heat flow between the working fluids, which was higher than that obtained with Case A and with the base model, as shown in Figure 12. This marked difference between the cases can be confirmed by comparing the heat flow of Case B (40.52 kW) and Case C (40.55 kW), with increases of 28.68 and 28.77%, respectively, considering the higher value of the mass flow analyzed.

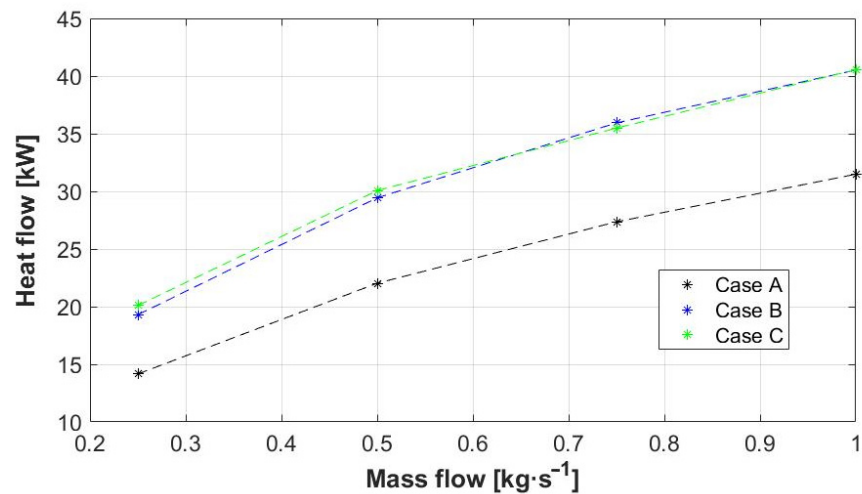


Figure 12. Heat flow for baffles with a 60° inclination in cases A, B, and C.

3.4. Changes in the Profile

Since the exchangers that incorporated baffles with an inclination of 60° with the ends oriented towards the cold fluid inlet and in an alternating manner presented a higher heat transfer, the models that were originally proposed with central tubes with circular profiles were used to analyze the heat flow with different profiles, considering a mass flow in the shell of $0.5 \text{ kg}\cdot\text{s}^{-1}$. For this study, a concept similar to the research developed by Olabi et al. [28] and Hadibafekr et al. [29] was considered, where the temperature change in the working fluid was studied with proposed cross sections incorporating various curvatures in the heat exchanger ducts.

3.4.1. Ellipse Profiles

An analysis of thermal energy flow in heat exchanger devices with profiles incorporating elliptical curves has been previously performed, as presented in the research of Andrade et al. [30]. However, the influence of this type of profile can vary according to the design of the exchanger analyzed, which is why, to determine the influence of the change in the heat flux present in the proposed device, a vertically and horizontally oriented ellipse-shaped profile was considered, as shown in Figure 13.

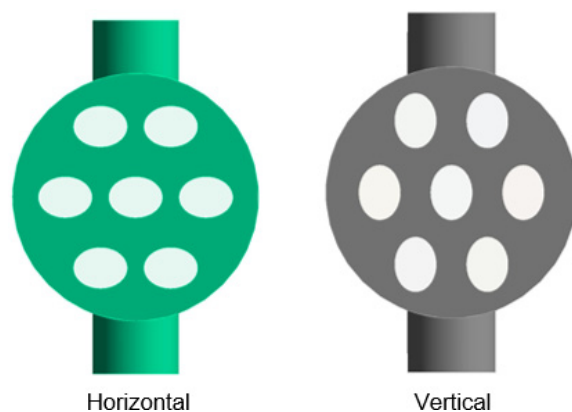


Figure 13. Internal tubes with elliptical profiles.

The analysis developed in the exchanger with horizontal elliptical profiles resulted in a higher heat flow in the device with inclined baffles and ends oriented towards the cold fluid outlet (Case B), compared to the baffles with alternating oriented ends (Case C), with a heat flow of 29.02 and 27.14 kW, respectively, as shown in Figure 14A. Similarly, when obtaining the results of the simulations of the heat exchangers with vertical elliptical profiles, it was determined that Case B (25.79 kW) generated a greater increase in heat flow when compared to Case C (24.15 kW), as shown in Figure 14B.

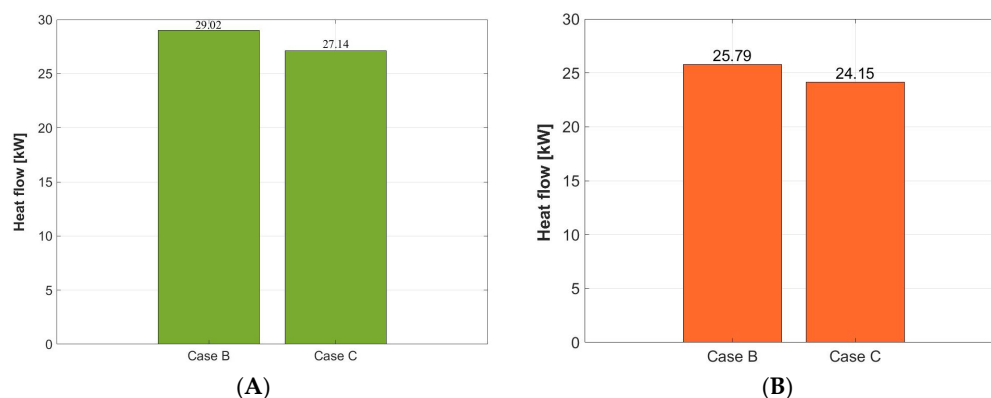


Figure 14. Heat flow considering horizontal (A) and vertical (B) elliptical profiles.

3.4.2. Profiles with Arches

As can be seen in studies such as those developed by Li et al. [8] and Abbasian et al. [10], the use of curvatures in the heat exchanger duct profiles generates an increase in heat flow. For this reason, as another alternative proposal to the circular profile in the outer zone, the behavior of the heat exchanger device was analyzed by incorporating profiles with four arches in the internal tubes in the outer part and circular inner profiles, as shown in Figure 15.

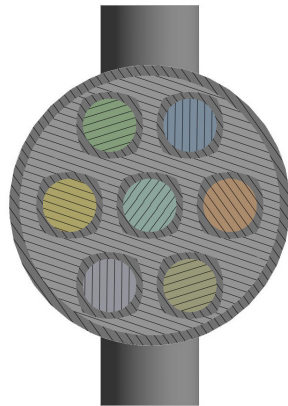


Figure 15. Internal tubes with arched profiles.

Similar to the study with elliptical profiles, simulations of the heat exchangers with arched profiles were carried out for the cases of baffles inclined at 60° with the ends oriented toward the cold fluid outlet (Case B) and alternately (Case C). When comparing the results of these cases, the presence of a higher heat flow in Case B (28.29 kW) was evident, as shown in Figure 16.

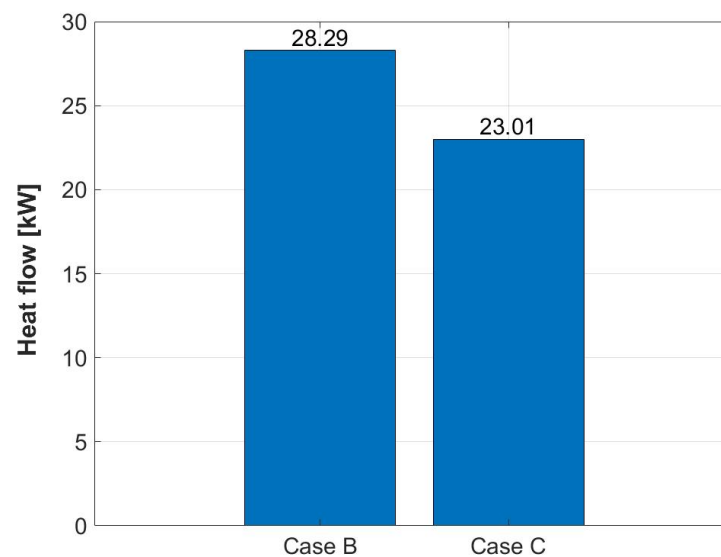


Figure 16. Heat flow considering arched profiles.

3.4.3. Octagonal Profiles

As a final change proposal for the heat exchanger internal tubes profiles and to show a higher heat flow in tubes with curved profiles, an octagonal profile was considered in the external area and a circular profile in the internal region of the tubes, as shown in Figure 17.

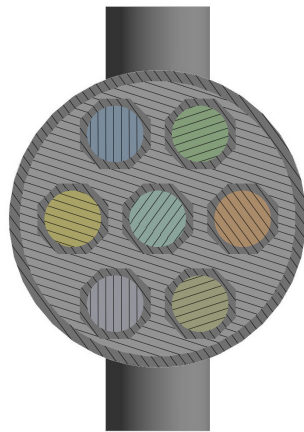


Figure 17. Inner tubes with octagonal profiles.

These profiles were analyzed under similar conditions as the previous cases, maintaining the inclination of the baffles and the orientation of their ends (Case B and C), generating, as a result, a higher heat flux for Case B (27.96 kW) than Case C (27.57 kW), with a reduced difference when compared to the previously simulated profiles, as presented in Figure 18.

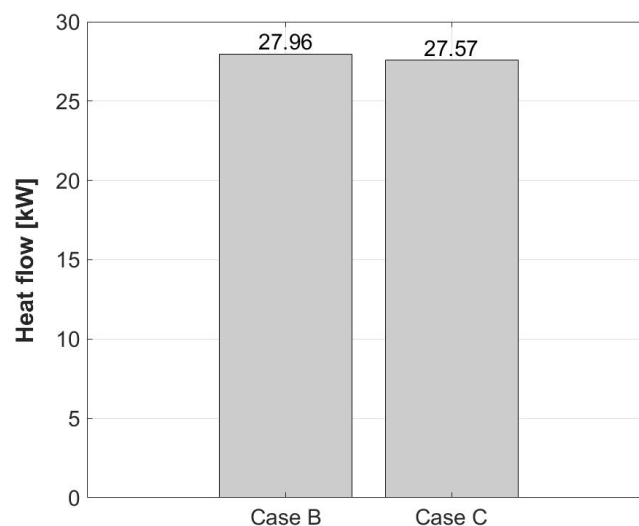


Figure 18. Heat flow considering octagonal profiles.

There was an increase in heat transfer in the fluids when varying the size of the baffle walls along with their inclination. This phenomenon may be associated with the directionality of the cold fluid inside the device by presenting a more extensive trajectory with greater contact with the surface of the hot fluid ducts [31], and with the possible presence of a greater amount of turbulence vortices in the areas adjacent to the baffle walls.

The change in the surface sections of the hot fluid ducts showed the influence on the orientation of the geometric shapes for the path of the fluid to be heated along with a change in the heat transfer that occurred by incorporating flat surfaces and a greater surface area of contact according to the geometric profile of the ducts.

4. Discussion

There was an increase in heat transfer in the fluids as the size of the baffle walls varied along with their inclination. This phenomenon may be associated with the directionality of the cold fluid inside the device as it presents a longer path with greater contact with the surface of the hot fluid ducts and the presence of turbulence vortices in the areas adjacent to the deflector walls.

The change in the surface sections of the hot fluid ducts showed the influence on the orientation of the geometric shapes with respect to the fluid path, along with a change in heat transfer that occurred when incorporating flat surfaces and a greater surface area of contact according to the geometric profile of the ducts.

The changes in the ducts' geometric shape demonstrated that this fact could influence the heat flux of the device which is directly proportional to the energy efficiency. A deeper analysis can determine a geometric shape able to generate a significant increase in the heat flux.

5. Conclusions

By developing the computational fluid dynamics analysis of various heat exchanger models and modifying geometrical parameters in their design, the following conclusions were obtained:

1. The influence of the increase in the height of the baffle walls concerning the internal diameter of the shell was shown with the heat exchange in the device where average cold fluid outlet temperatures of 27.42, 29.51, and 31.91 °C were obtained for baffles with 25, 50, and 75% of the height, respectively.
2. The inclination of the deflector walls that generated the greatest temperature difference in the device was 60° for the horizontal axis, with heat fluxes of 29.44 and 30.07 kW for the ends oriented towards the cold fluid outlet and alternating, respectively. This demonstrates the positive influence of the baffles' inclination in a higher heat transfer process.
3. The heat flux in a heat exchanger is directly proportional to the energy efficiency, considering that the lowest heat flux (24.15 kW) was generated by the combination of profiles with an elliptical shape vertically oriented and baffle walls with an inclination of 60°. This means that the combination cannot be recommended.
4. The duct's geometric shape that generated the greatest temperature difference between the inlets and outlets of the device, expressed by an increase in heat flow (29.02 kW), was the one that incorporated baffle walls with an inclination of 60° with the ends oriented toward the cold fluid outlet with a horizontal elliptical profile on the inner tubes.
5. Comparing the highest heat fluxes obtained by the changes in the baffles' inclination (29.44–30.07 kW) with the best heat flux presented in the combination of baffle inclination and different duct shape (29.02 kW), the baffle inclination emerges as the strongest geometric factor in the energy efficiency of the heat exchanger.

Author Contributions: J.E.-C. and W.Q.: conceptualization, methodology, validation, and writing—review and editing. W.Q. and C.N.-L.: conceptualization, methodology, software, and writing—original draft. P.Q.: data curation and formal analysis. W.Q. and C.N.-L.: supervision, and validation. W.Q. and J.E.-C.: writing—review and editing. All authors have read and agreed to the published version of the manuscript.

Funding: This work was financially funded by the Engineering, Productivity, and Industrial Simulation Research Group (GIIPSI) of the Universidad Politécnica Salesiana and Salesian Institutions of Higher Education (IUS).

Data Availability Statement: The data presented in this study are available on request from the corresponding author. The data are not publicly available due to future research.

Acknowledgments: The Universidad Politécnica Salesiana and Universidad Pontificia Bolivariana supported this work via the Engineering, Productivity, and Industrial Simulation Research Group (GIIPSI).

Conflicts of Interest: The authors declare no conflicts of interest.

Nomenclature

Symbol	Description
ρ	Density; [$\text{kg}\cdot\text{m}^{-3}$]
t	Time; [s]
V	Velocity; [$\text{m}\cdot\text{s}^{-1}$]
S_m	Mass source; [$\text{kg}\cdot\text{m}^{-3}\cdot\text{s}^{-1}$]
P	Pressure; [Pa]
μ	Dynamic viscosity; [$\text{Pa}\cdot\text{s}$]
F	Force; [N]
E	Total energy; [J]
∇	Grad operator
S_h	Defined energy source; [$\text{W}\cdot\text{m}^{-3}$]
J	Mass flow; diffusion flow; [$\text{kg}\cdot\text{m}^{-2}\cdot\text{s}^{-1}$]
k	Kynetic energy turbulence; [$\text{m}^2\cdot\text{s}^{-2}$]
u	Velocity magnitude; [$\text{m}\cdot\text{s}^{-1}$]
x	Axial coordinate
μ_t	Dynamic turbulence viscosity; [$\text{kg}\cdot\text{m}^{-1}\cdot\text{s}^{-1}$]
σ_k	Prandtl turbulence number
G_k	Kinetic turbulence energy generation
G_b	Flotability kinetic turbulence energy generation
ϵ	Disipation rate; [$\text{m}^2\cdot\text{s}^{-3}$]
S_k	Kinetic turbulence source; [$\text{kg}\cdot\text{m}^{-1}\cdot\text{s}^{-3}$]

References

- Gupta, S.K.; Verma, H.; Yadav, N. A review on recent development of nanofluid utilization in shell & tube heat exchanger for saving of energy. *Mater. Today Proc.* **2021**, *54*, 579–589. [[CrossRef](#)]
- Mediaceja, Y.R.; Alfonso, H.L.L.; Sánchez-Escalona, A.A.; Camaraza-Medina, Y.; Corrales, M.F.S.; Urgelles, M.L.; Leyva, E.G. Análisis termoenergético del sistema de generación de vapor de una central térmica de 49 MW. *Enfoque UTE* **2020**, *11*, 87–101. [[CrossRef](#)]
- Lara-Montaño, O.D.; Gómez-Castro, F.I.; Gutiérrez-Antonio, C. Comparison of the performance of different metaheuristic methods for the optimization of shell-and-tube heat exchangers. *Comput. Chem. Eng.* **2021**, *152*, 107403. [[CrossRef](#)]
- Ünverdi, M. Prediction of heat transfer coefficient and friction factor of mini channel shell and tube heat exchanger using numerical analysis and experimental validation. *Int. J. Therm. Sci.* **2022**, *171*, 107182. [[CrossRef](#)]
- Ravikumar, M.; Raj, Y.A. Investigation of fin profile on the performance of the shell and tube heat exchanger. *Mater. Today Proc.* **2021**, *45*, 7910–7916. [[CrossRef](#)]
- Pereira, I.P.; Bagajewicz, M.J.; Costa, A.L. Global optimization of the design of horizontal shell and tube condensers. *Chem. Eng. Sci.* **2021**, *236*, 116474. [[CrossRef](#)]
- Yang, Z.; Ma, Y.; Zhang, N.; Smith, R. Optimization of Shell and Tube Heat Exchangers Sizing with Heat Transfer Enhancement. *Comput. Aided Chem. Eng.* **2020**, *48*, 937–942. [[CrossRef](#)]
- Li, X.; Wang, L.; Feng, R.; Wang, Z.; Liu, S.; Zhu, D. Study on shell side heat transport enhancement of double tube heat exchangers by twisted oval tubes. *Int. Commun. Heat Mass Transf.* **2021**, *124*, 105273. [[CrossRef](#)]
- Bahiraie, M.; Naseri, M.; Monavari, A. A CFD study on thermohydraulic characteristics of a nanofluid in a shell-and-tube heat exchanger fitted with new unilateral ladder type helical baffles. *Int. Commun. Heat Mass Transf.* **2021**, *124*, 105248. [[CrossRef](#)]
- Arani, A.A.A.; Uosofvand, H. Double-pass shell-and-tube heat exchanger performance enhancement with new combined baffle and elliptical tube bundle arrangement. *Int. J. Therm. Sci.* **2021**, *167*, 106999. [[CrossRef](#)]
- Ren, H.; He, M.; Lin, W.; Yang, L.; Li, W.; Ma, Z. Performance investigation and sensitivity analysis of shell-and-tube phase change material thermal energy storage. *J. Energy Storage* **2020**, *33*, 102040. [[CrossRef](#)]
- Quitiaquez, W.; Estupinan-Campos, J.; Isaza-Roldan, C.A.; Nieto-Londono, C.; Quitiaquez, P.; Toapanta-Ramos, F. Numerical simulation of a collector/evaporator for direct-expansion solar-assisted heat pump. In Proceedings of the 2020 IEEE ANDESCON, Quito, Ecuador, 13–16 October 2020; pp. 1–6.
- Li, N.; Chen, J.; Cheng, T.; Klemeš, J.J.; Varbanov, P.S.; Wang, Q.; Yang, W.; Liu, X.; Zeng, M. Analysing thermal-hydraulic performance and energy efficiency of shell-and-tube heat exchangers with longitudinal flow based on experiment and numerical simulation. *Energy* **2020**, *202*, 117757. [[CrossRef](#)]
- El-Said, E.M.; Elsheikh, A.H.; El-Tahan, H.R. Effect of curved segmental baffle on a shell and tube heat exchanger thermohydraulic performance: Numerical investigation. *Int. J. Therm. Sci.* **2021**, *165*, 106922. [[CrossRef](#)]
- Biçer, N.; Engin, T.; Yaşar, H.; Büyükkaya, E.; Aydın, A.; Topuz, A. Design optimization of a shell-and-tube heat exchanger with novel three-zonal baffle by using CFD and taguchi method. *Int. J. Therm. Sci.* **2020**, *155*, 106417. [[CrossRef](#)]

16. Elmekawy, A.M.N.; Ibrahim, A.A.; Shahin, A.M.; Al-Ali, S.; Hassan, G.E. Performance enhancement for tube bank staggered configuration heat exchanger—CFD Study. *Chem. Eng. Process. Process Intensif.* **2021**, *164*, 108392. [[CrossRef](#)]
17. Vivekanandan, M.; Saravanan, G.; Vijayan, V.; Gopalakrishnan, K.; Krishna, J.P. Experimental and CFD investigation of spiral tube heat exchanger. *Mater. Today Proc.* **2020**, *37*, 3689–3696. [[CrossRef](#)]
18. Kola, P.V.K.V.; Pisipaty, S.K.; Mendu, S.S.; Ghosh, R. Optimization of performance parameters of a double pipe heat exchanger with cut twisted tapes using CFD and RSM. *Chem. Eng. Process. Process Intensif.* **2021**, *163*, 108362. [[CrossRef](#)]
19. Aliaga, D.; Feick, R.; Brooks, W.; Mery, M.; Gers, R.; Levi, J.; Romero, C. Modified solar chimney configuration with a heat exchanger: Experiment and CFD simulation. *Therm. Sci. Eng. Prog.* **2021**, *22*, 100850. [[CrossRef](#)]
20. Vivekanandan, M.; Venkatesh, R.; Periyasamy, R.; Mohankumar, S.; Devakumar, L. Experimental and CFD investigation of helical coil heat exchanger with flower baffle. *Mater. Today Proc.* **2020**, *37*, 2174–2182. [[CrossRef](#)]
21. Wen, T.; Lu, L.; He, W.; Min, Y. Fundamentals and applications of CFD technology on analyzing falling film heat and mass exchangers: A comprehensive review. *Appl. Energy* **2020**, *261*, 114473. [[CrossRef](#)]
22. Quitiaquez, W.; Estupiñán-Campos, J.; Nieto-Londoño, C.; Quitiaquez, P. CFD Analysis of Heat Transfer Enhancement in a Flat-Plate Solar Collector/Evaporator with Different Geometric Variations in the Cross Section. *Energies* **2023**, *16*, 5755. [[CrossRef](#)]
23. Chihab, Y.; Garoum, M.; Laaroussi, N. Dynamic thermal performance of multilayer hollow clay walls filled with insulation materials: Toward energy saving in hot climates. *Energy Built Environ.* **2024**, *5*, 70–80. [[CrossRef](#)]
24. Wang, Z.; Suen, K. Numerical comparisons of the thermal behaviour of air and refrigerants in the vortex tube. *Appl. Therm. Eng.* **2020**, *164*, 114515. [[CrossRef](#)]
25. Jiang, H.; Niu, F.; Ma, Q.; Su, W.; Wang, E.; He, J. Numerical analysis of heat transfer between air inside and outside the tunnel caused by piston action. *Int. J. Therm. Sci.* **2021**, *170*, 107164. [[CrossRef](#)]
26. Elgendy, H.; Czernski, K. Numerical Study of Flow and Heat Transfer Characteristics in a Simplified Dual Fluid Reactor. *Energies* **2023**, *16*, 4989. [[CrossRef](#)]
27. Arsenyeva, O.; Tovazhnyanskyy, L.; Kapustenko, P.; Klemeš, J.J.; Varbanov, P.S. Review of Developments in Plate Heat Exchanger Heat Transfer Enhancement for Single-Phase Applications in Process Industries. *Energies* **2023**, *16*, 4976. [[CrossRef](#)]
28. Olabi, A.; Wilberforce, T.; Sayed, E.T.; Elsaid, K.; Rahman, S.A.; Abdelkareem, M.A. Geometrical effect coupled with nanofluid on heat transfer enhancement in heat exchangers. *Int. J. Thermofluids* **2021**, *10*, 100072. [[CrossRef](#)]
29. Hadibafekr, S.; Mirzaee, I.; Khalilian, M.; Shirvani, H. Thermohydraulic performance intensification of lobed heat exchangers using tube axis corrugation: Numerical assessment on geometrical configurations. *Chem. Eng. Process. Process Intensif.* **2022**, *171*, 108763. [[CrossRef](#)]
30. Cando, A.X.A.; Sarzosa, W.Q.; Toapanta, L.F. CFD Analysis of a solar flat plate collector with different cross sections. *Enfoque UTE* **2020**, *11*, 95–108. [[CrossRef](#)]
31. Quitiaquez, P.; Cocha, J.; Quitiaquez, W.; Vaca, X. Investigation of geometric parameters with HSS tools in machining polyamide 6 using Taguchi method. *Mater. Today Proc.* **2022**, *49*, 181–187. [[CrossRef](#)]

Disclaimer/Publisher’s Note: The statements, opinions and data contained in all publications are solely those of the individual author(s) and contributor(s) and not of MDPI and/or the editor(s). MDPI and/or the editor(s) disclaim responsibility for any injury to people or property resulting from any ideas, methods, instructions or products referred to in the content.